Toronto Metropolitan University

AE/ME 8115 Finite Element Methods in Engineering.
Final Report

Design and Finite Element Analysis of an Aircraft Wing with Ribs, Spars, and Stringers.

Student Name: Aman Gilani

Student No.: 500879895

Program: Aerospace Engineering.

Abstract

The structural design and analysis of an aircraft wing are two of the most important aspects of the modern aviation industry. A strong wing design ensures the safety of the passengers and enhances the aircraft's performance while reducing the cost per flight for the consumers. Therefore, this project focuses on the design aspects and analysis of the Cessna 152 wing structure. The Cessna 152 wing structure comprises on ribs, spars and stringers that undergo various aerodynamic and structural loads. Using the current resources available, a 3D CAD model of the wing structure was developed on SolidWorks and subjected to a Finite Element Analysis on Ansys static structural. The analysis considered key loads, including maximum wing loading, structural distribution and localized fuel distribution along with the appropriate boundary conditions for Cessna 152. The primary objective of this project was to computationally determine the maximum wing deflection, and the internal forces (stress and strain) within each structural element. The wing structural model was meshed using two different element types, namely linear and quadratic tetrahedron elements, and 4 different grid sizes for each element. For the four grid sizes, its respective computation yield deformation, stress and strain values which is used to compute a grid independent solution. The maximum deformation was calculated to be 0.020358 m and 0.014292 m for quadratic and linear tetrahedron elements respectively. The maximum stress was calculated to be 1.1564e+8 and 4.7931e+8 for linear and quadratic tetrahedron elements respectively. Comparing these results against material properties it was verified that the wing's failure loads are well beyond what it achieves during this static structural analysis. This comprehensive analysis aims to ensure the robustness, efficiency, and safety of the wing design under operational conditions.

Table of Contents

List of Figures

List of Tables

1. Introduction and Literature Review

An aircraft wing is a fin type structure that promotes necessary lift generation for the aircraft to achieve and maintain a steady, level flight. Therefore, the design and analysis of its internal structure becomes an important aspect in the overall wing design. Given the wing's primary goal to produce the necessary lift, its internal structure supports the majority of aerodynamic loading to ensure the structural integrity of the aircraft. A typical wing structure comprises of ribs, spars and stringers along its wingspan, which endures various loads during the flight envelope. Some examples of wing loading include, lift forces and moments, structural weight, engine weight, and fuel weight. Therefore, the wing structure must be designed to withstand a combination of these forces plus the aerospace safety factor of 1.5 to ensure utmost safety and reliability of the aircraft in service.

This project proposes a comprehensive design and analysis of the Cessna 152 wing structure with ribs, spars and stringers. The main objective of this project is to assess the structural strength in terms of wing deflection and element forces to ensure the robustness of the design process. By researching the Cessna 152 wing structure, creating a 3D CAD model of its wing structure and applying a simplified set of load and boundary conditions, this analysis will provide insights into the wing's performance under ultimate stresses. The key loads acting on the wing structure includes the maximum wing loading along its wingspan, the weight of its structure distributed along the wingspan, and a localized fuel weight over the fuel tank area. The boundary conditions for this analysis are parallel to that of a high wing Cessna 152 aircraft. The wings are bolted to its respective side of the fuselage around the leading and trailing edge plus the wing strut is also bolted from the wing to the lower part of the fuselage.

The primary objectives of the FEA analysis are to determine the maximum wing deformation and to calculate the forces within each structural element. These results will be compared against material properties to verify the wing's failure loads, thus establishing a theoretical limit loading for the wing design. The pre-processing step of the analysis includes a detailed design of the 3D CAD model of the structure. Following this, the discretization of the model into finite elements is completed. This process is also known as meshing, which includes defining the mesh size, type and quality on Ansys Static Structural. Next, the material properties for each element are defined. The last step of pre-processing is defining the loading and boundary conditions on the model. Post-processing, the force and deformation results are studied and verified to ensure that the aircraft wing design is both robust, efficient, and capable of withstanding operational loads while minimizing weight and material usage.

2. Wing Structure Design

The design stage for this project integrates the geometry and the material properties of a Cessna 152 wing structure within a SolidWorks assembly model. A half span Cessna 152 wing structure comprises of 11 ribs, 2 spars and 6 stringers. This section of the report focuses on the design of these components. **Figure 1** below illustrates a hand drawing of the overall wing geometry. The figure illustrates the station of each rib along the wingspan. The figure also illustrates the connection point of the wing struct with the wing leading edge spar.

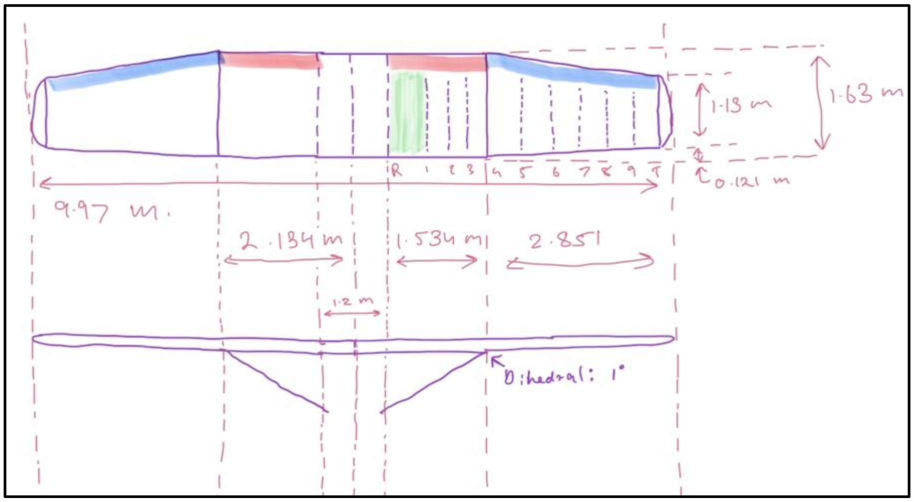

Figure 1: *Wing Dimensions with Rib locations.*

As illustrated in **Figure 1**, the wing has a total wingspan of 9.97 m, with a root chord of 1.63 m and a tip chord of 1.13 m. The overall wing dimensions are tabulated in **Table 1.**

Table 1: *Cessna Wing Parameters.*

Parameter	**Dimension**
Airfoil Shape	NACA 2412
Wing Area	14.59 m2
Wingspan	9.97 m
Root Chord	1.63 m
Tip Chord	1.13 m
Wing Aspect Ratio	6.7
Wing Incidence Angle	1^{o} at Root, 0^{o} at tip

2.1 Airfoil and Ribs

The wing airfoil shape for a Cessna 152 aircraft is designed with a NACA 2412 airfoil. The airfoil features a maximum thickness of 12% at 30% chord length and a maximum chamber of 2% at the 40% chord length location. This NACA 2412 cross-section is illustrated in **Figure 2**. The NACA 2412 airfoil shape is incorporated into each and every rib of the wing structure to have an overall uniform and well-defined wing contour.

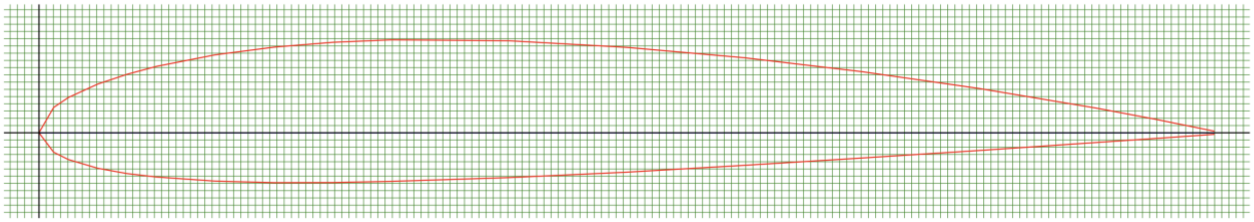

Figure 2: *NACA 2412 Airfoil Cross-section.*

As seen in **Figure 3** the half span consists of 11 ribs. The influence of the tapper ratio and wing incidence angle causes the ribs to have different chord lengths at each station. The chord length for each rib is tabulated in **Table 2.** The location of each rib with respect to the wing root rib is also tabulated in **Table 2**. The location of the first rib after the root incorporates the length of the fuel tank, after which the spacing remains constant for the rectangular shape, and taper shape respectively.

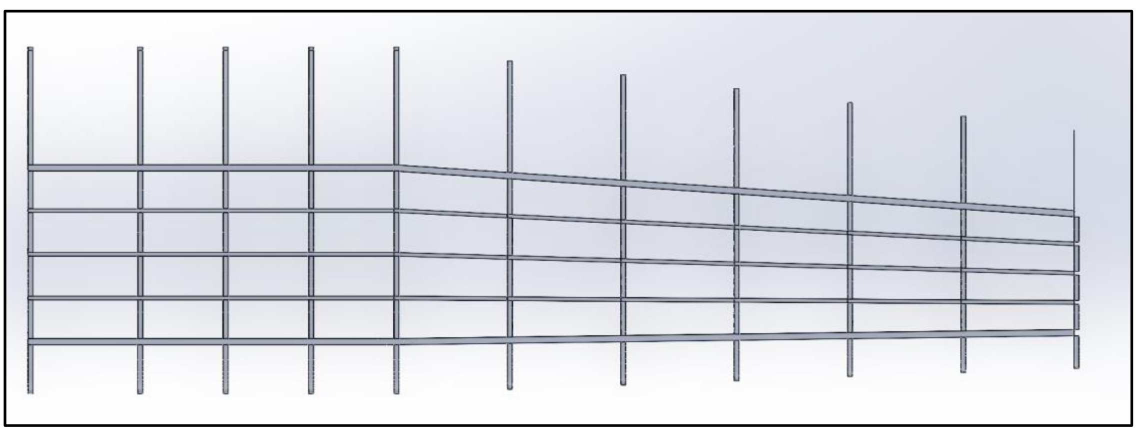

Figure 3: *Rib Locations (Wing Top View).*

Table 2: Rib Chord Length along Half Wingspan.

Rib	Chord length	Location
Root Rib	1.63 m	0
Rib 1	1.63	0.45
Rib 2	1.63	0.81
Rib 3	1.63	1.17
Rib 4	1.63	1.53
Rib 5	1.56	2.01
Rib 6	1.47	2.48
Rib 7	1.39	2.96
Rib 8	1.30	3.43
Rib 9	1.21	3.91
Tip Rib	1.13	4.38

The rib structure for the Cessna 152 aircraft integrates a C-shape cross-section. The C-shape rib cross-section features a higher strength tolerance while reducing the thickness and weight of the rib structure. The ribs tolerate all transverse loads from stringers and transfer them to the two wide flange beams called spars that are designed to take transverse shear loads. The rib cross-sectional shape is illustrated in **Figure 4.** The cross-sectional dimensions of the rib structure are tabulated in **Table 3.**

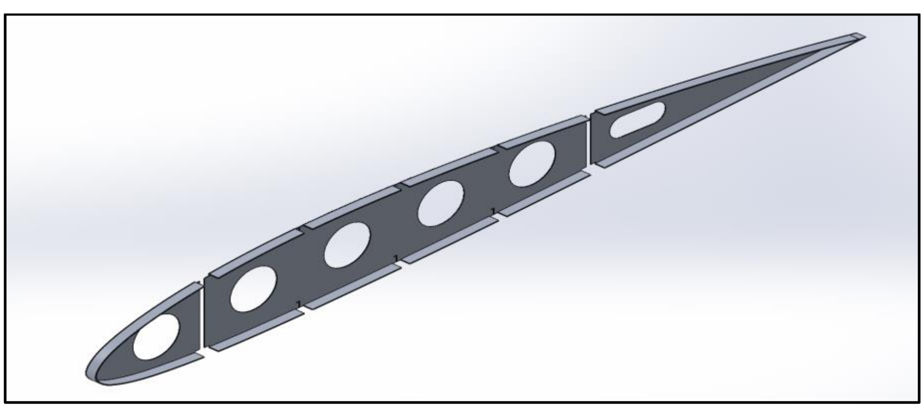

Figure 4: Rib Shape.

Table 3: *Rib Cross-section Dimension.*

Parameter	Dimension
Thickness	0.005 m
Flange Thickness	0.0025 m
Flange Width	0.01 m

2.2 Spars

Spars are the principal structural members of the wing. The Cessna 152 wing design integrates 2 spars along its wingspan, making the model a multi-spar design. The spars are designed to tolerate both, transverse and shear loads from other structural members of the wing. The leading-edge spar is located at 15% chord length for each rib. The trailing edge spar is located at 65% chord length for each rib. The overall spar shape is illustrated in **Figure 5.**

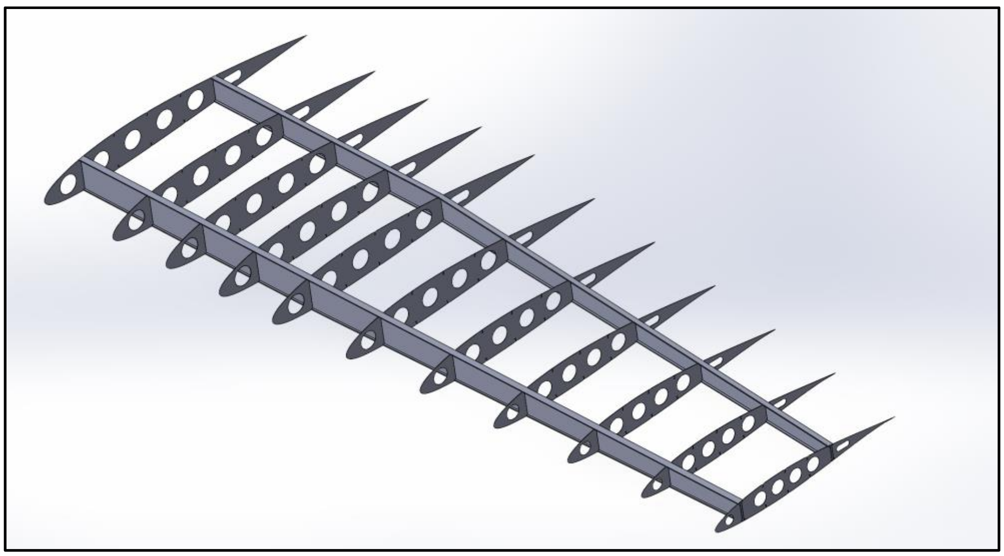

Figure 5*: Wing Structure with Ribs and Spars.*

The leading-edge spar structure features an I-Type cross-section, whereas the trailing edge spar features a C-Type cross-section. The cross-sectional dimensions for the leading edge and trailing edge spar are tabulated in **Table 4.** The spar cross-sectional is presented in **Figure 6.**

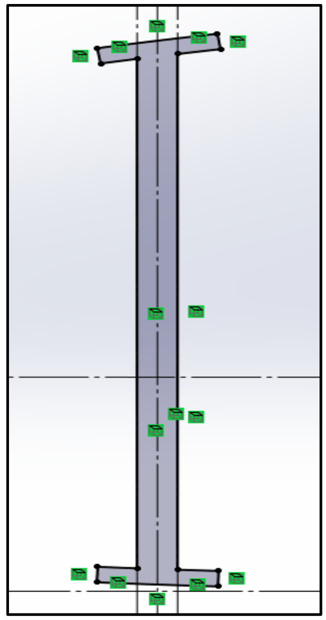

Figure 6: *Leading Edge Spar Cross-Section.*

Table 4: *Spar Cross-Sectional Dimensions.*

	Parameter	**Dimension**
Leading Edge Spar	Length ‘a’	0.176 m
	Spar cap Length ‘b’	0.003 m
	Spar cap Thickness ‘c’	0.005 m
Trailing Edge Spar	Length ‘a’	0.132 m
	Spar cap Length ‘b’	0.003 m
	Spar cap Thickness ‘c’	0.005 m

2.3 Stringers

Lastly, the stringers are structural component that run parallel to the spars. They are designed to tolerate maximum bending capacity. The stringer serves the purpose of transferring loads from the wing’s skin to the ribs. The Cessna 152 wing consists of 6 stringers, 3 at the top and 3 at the bottom. Each stringer is located equi-spaced to each other within the two spars as seen in **Figure 7.**

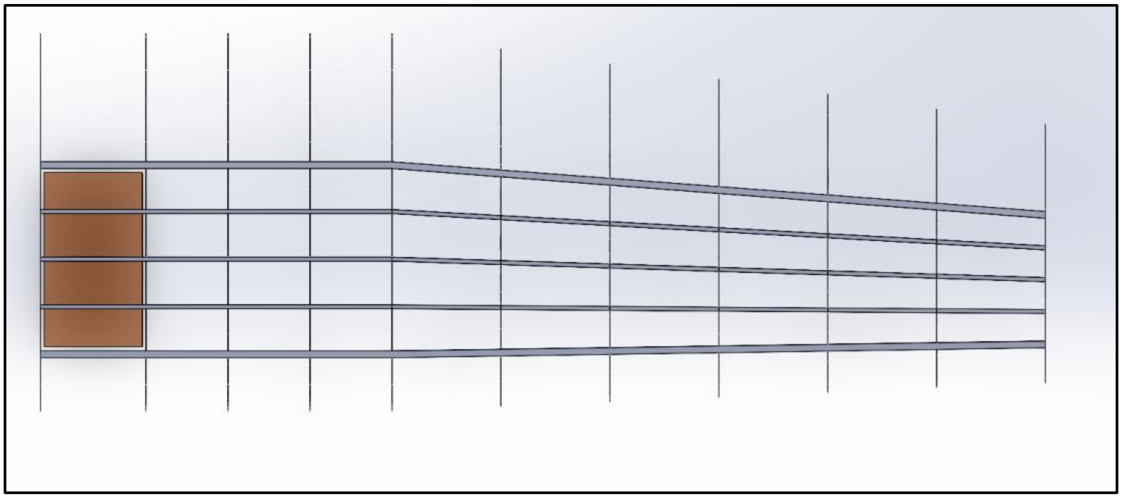

Figure 7: *Top View of Cessna 152 Wing Structure.*

The stringer cross-section features a J-type shape. The cross-sectional dimensions for the stringer are tabulated in **Table 5**. The J-stringer cross-section is illustrated in **Figure 8.**

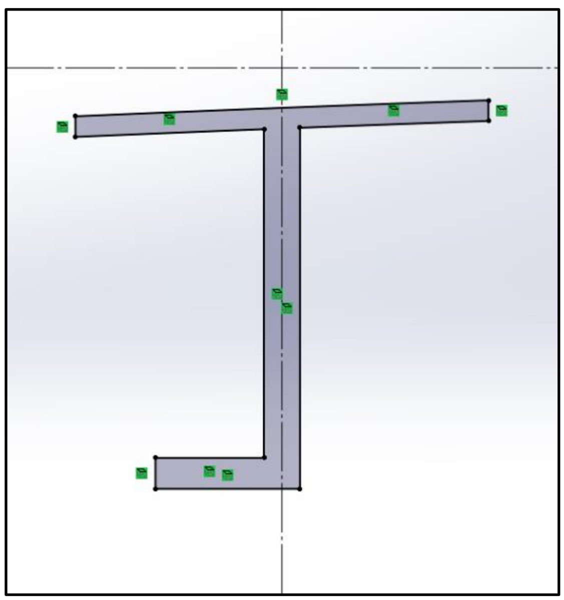

Figure 8: *J-Stringer Cross-Section.*

Table 5: Stringer Cross-Sectional Dimensions.

Parameter	Dimension
t_a	0.0009 m
t_f	0.0013 m
t_w	0.0016 m
b_w	0.0156 m
b_f	0.0062 m
b_a	0.0089 m

2.4 Material Selection

The Cessna 152 wing structure is made from Aluminium 2024-T4 alloy. This material is applied to all the elements: spars, ribs and stringers, during the preprocessing procedure on Ansys. The following **Table 6** tabulates the material properties for Aluminium 2024-T4 alloy.

Table 6: Aluminium 2024-T4 Material Property.

Parameter	Dimension
Elastic Modulus	72.4 GPa
Poisson's Ratio	0.33
Shear Modulus	28 GPa
Mass Density	2780 Kg/m^3
Tensile Strength	470 MPa
Yield Strength	325 MPa

3. CAD Modelling

The next section of this report focusses on outlining the development of the 3D CAD model of the wing structure within SolidWorks assembly and defining the appropriate force and boundary conditions on the model as a pre-processing step for Ansys static structural analysis. Using the geometry and dimension described in the previous section, a CAD model is developed on SolidWorks. Each element is saved as a separate body in the overall assembly geometry, following which the joint contact is defined between each element. The wing structural model is developed this way because each the rib, spar, and stringer are maintained as separate elements and thus undergoes dissimilar deflection, stress and strain. After developing the CAD model on SolidWorks, the assembly file containing the model is exported to Ansys as a STEP file type. This format retains the solid nature of each element, for us to apply the appropriate material properties before meshing.

3.1 Mesh Size, Quality, and Element Type

The next pre-processing step is defining an acceptable mesh for the wing structural geometry. Defining an acceptable mesh size, quality, and method allows for the geometry to have a non-intersecting, clean mesh, thus reducing computational errors. For this project, four different mesh sizes were used for two different element types. **Table 7** below tabulates this data for each mesh size. Additionally, to the mesh size, the table tabulates the number of nodes, and number of elements for each respective mesh. Lastly, for each mesh size, a linear tetrahedron and a quadratic tetrahedron element type is used for the analysis. The first mesh is with a coarse size of 0.02 m, and the last mesh is the finest for this study with a size of 0.0075 m for the ribs, spars, and stringers. The finer the mesh is, it can capture accurate details of the geometry and stress gradients, leading to more precise result which are necessary to accurately represent a complex model.

Table 7: *Mesh size, No. of Nodes, and No. of Elements for each Mesh.*

		Mesh 1	Mesh 2	Mesh 3	Mesh 4
Size	Ribs and Spars (m)	0.02	0.00925	0.009	0.0075
	Stringers (m)	0.02	0.0095	0.009	0.0075
No. of Nodes		450,975	896,147	969,282	1,294,362
No. of Elements		189,103	343,497	371,455	504,537
Element Type		Linear and Quadratic Tetrahedron Elements			

The **Figure 9** below illustrates the trend between number of elements and its respective mesh size. Note that the x-axis of the graph denotes the mesh number and not the actual size, the mesh size is tabulated in **Table 7**. As expected, the number of elements increases as the mesh size decreases. Thus, indicating that the finest mesh size will yield the most accurate result. The meshes developed on Ansys for each size are illustrated in Figures 15,16,17 and 18 in the appendix section.

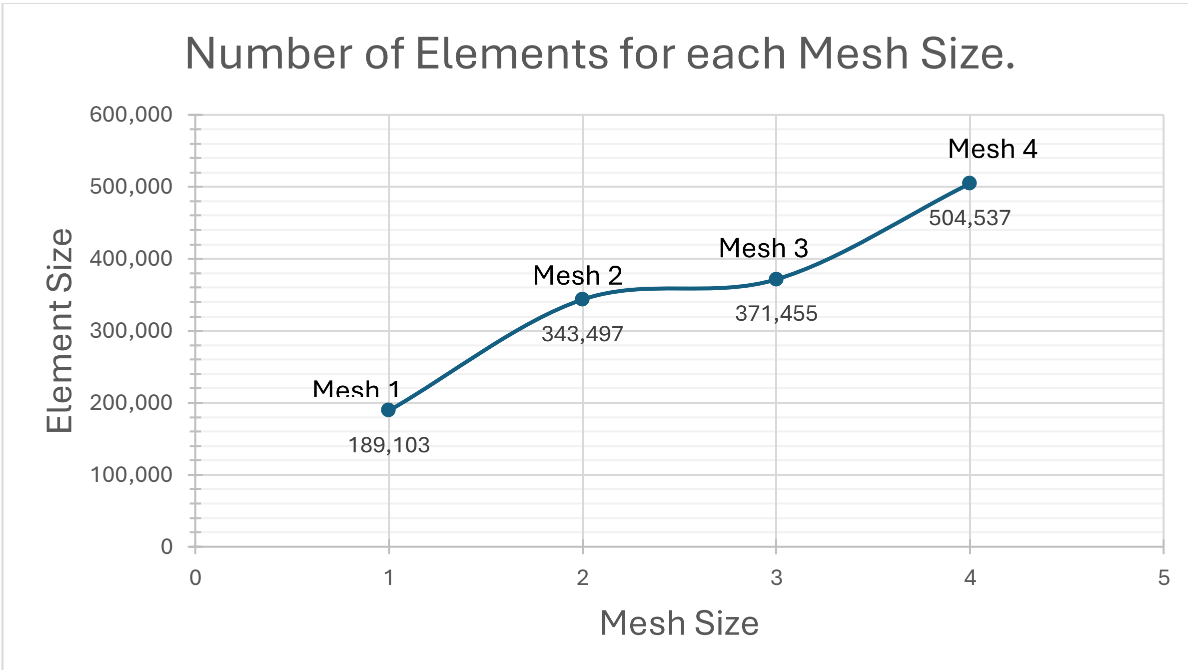

Figure 9: *Number of Elements for each Mesh Size.*

3.2 Forces and Boundary conditions

After completing the meshing process on Ansys, the following boundary and force conditions are used to conduct a static structural analysis. The wing's root rib is bolted to its respective side of the fuselage around the leading and trailing edge plus the wing strut is also bolted from the wing to the lower part of the fuselage. These connections can be modelled as bolted joints. However, to simplify the analysis further, the two bolt joints at the root rib are modelled as fixed support. The bolt joint at the wing strut is modelled as a pin joint to allow for a rotational motion. This simplification is done because calculating the bolt forces is not in the scope of this project.

Table 8: *Loading Boundary Conditions*

Parameter	Dimension	Location
Structural Weight (half span)	140 N/m^2	Linear distribution, over the Half Wingspan
Max Wing Loading (half span)	513 N/m^2	Linear distribution, over the Half Wingspan
Fuel Loading	705.6 N	Linear distribution, between root rib and the second rib.

The key loads acting on the wing structure includes the maximum wing loading along its wingspan, the weight of its structure distributed along the wingspan, and a localized fuel weight over the fuel tank area. **Table 8** above tabulates the loading and its location. After applying the above-mentioned material properties to the spars, ribs and stringers, the total weight of the half span wing structure was calculated to be 50 Kg. The linear distributed force applied on the wing model on Ansys accounts for an additional 1.5 safety factor.

4. Simulation Results

Following the completion of all preprocessing steps, the wing structure system is solved using an isotropic elasticity material model. This model only requires the Young's modulus and the Poisson's ratio to calculate the system deformations, stress and strain values. The model simulates the wing structure with an isotropic material assigned with a linear elastic behaviour. The results presented and evaluated for this simulation study includes maximum system deformation, maximum equivalent (Von-Mises) stress, maximum equivalent (Von-Mises) strain, maximum principle stress, maximum sheer stress and maximum normal stress.

The following **Table 9** tabulates the static structural simulation results for a linear tetrahedron element type and for four different mesh sizes.

Table 9: *Static Structural Results for Linear Tetrahedron Elements.*

Mesh Size	Max Deformation (m)	Max Equivalent Elastic Strain (m/m)	Max Equivalent Stress (Pa)
Mesh 1	0.010907	0.0047474	2.7568e+8
Mesh 2	0.014222	0.0044213	3.1576e+8
Mesh 3	0.014194	0.0044585	2.5915e+8
Mesh 4	0.014292	0.0032642	1.1564e+8

As seen in **Figure 10**, for a linear tetrahedron element type, the maximum deformation increases and converges to a steady value as the mesh refines. Whereas, the maximum elastic strain, and maximum equivalent stress follow a decreasing linear trend as the mesh size is reduced. This trend is expected, since a finer mesh can accurately compute the stress and strain in the geometry for the given boundary and force conditions. Note that the two y-axes for **Figure 10** are in different scales. The left y-axis represents the strain while the right y-axis represents the stress function. The stress and strain results for linear tetrahedron element for all grid sizes are presented in the appendix section.

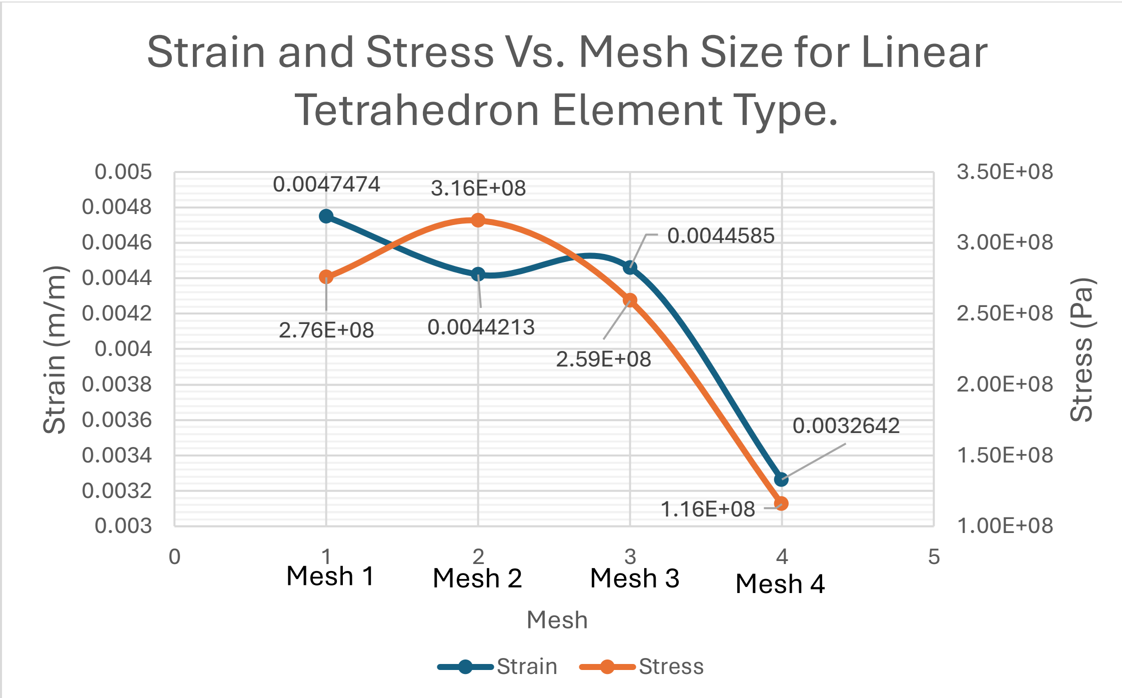

Figure 10: *Strain and Stress Vs. Mesh Size for Linear Tetrahedron Element Type.*

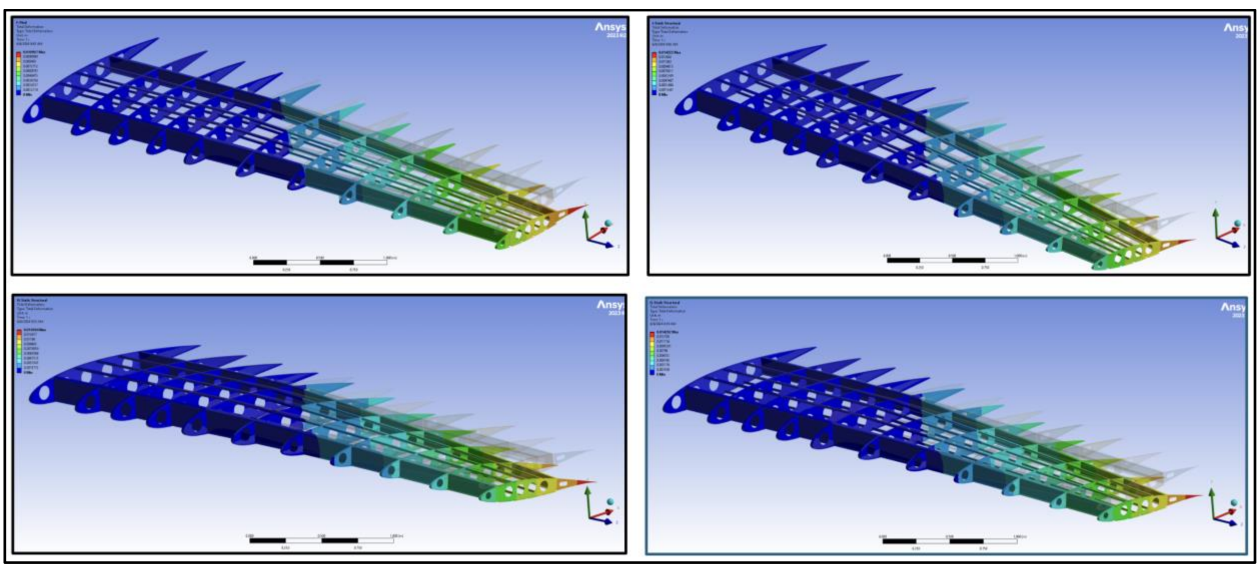

Figure 11: *Total Deformation Results for each Grid size. (Top Left: Grid 1, Top Right: Grid 2, Bottom Left: Grid 3, Bottom Right: Grid 4.)*

The **Figure 11** illustrates the total deformation results for each grid size for the linear tetrahedron element. The following **Table 10** tabulates the static structural simulation results for a quadratic tetrahedron element type and for four different mesh sizes.

***Table 10**: Static Structural Results for Quadratic Tetrahedron Elements.*

Mesh Size	Max Deformation (m)	Max Equivalent Elastic Strain (m/m)	Max Equivalent Stress (Pa)
Mesh 1	0.018588	0.013673	8.1367e+8
Mesh 2	0.019892	0.011177	4.4043e+8
Mesh 3	0.020272	0.010263	3.8838e+8
Mesh 4	0.020358	0.010911	4.7931e+8

As seen in **Figure 12**, for a quadratic tetrahedron element type, the maximum deformation increases and converges to a steady value as the mesh refines. Whereas, the maximum elastic strain, and maximum equivalent stress follow a quadratic function as the mesh size is reduced. This trend is expected, since a finer mesh can accurately compute the stress and strain in the geometry for the given boundary and force conditions. Note that the two y-axes for **Figure 12** are in different scales. The left y-axis represents the strain while the right y-axis represents the stress function. The stress and strain results for quadratic tetrahedron element for all grid sizes are presented in the appendix section.

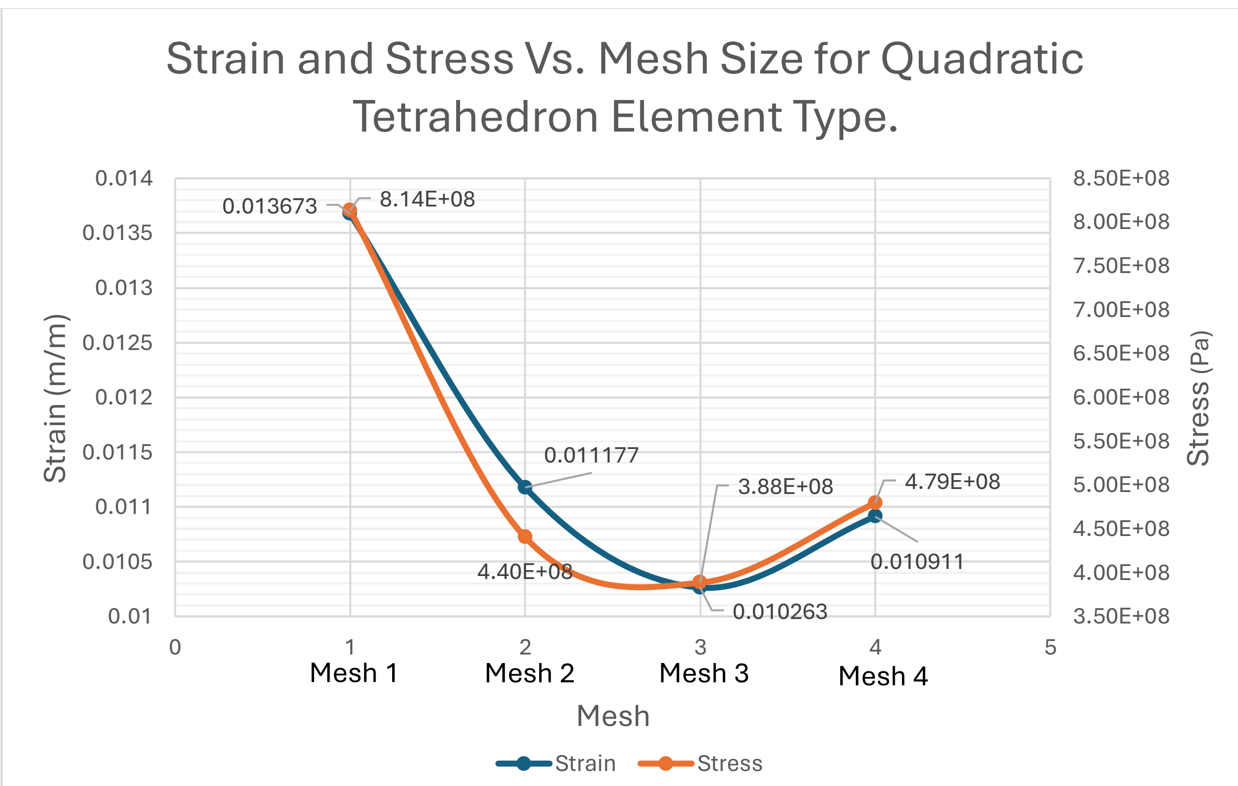

***Figure 12:** Strain and Stress Vs. Mesh Size for Quadratic Tetrahedron Element Type.*

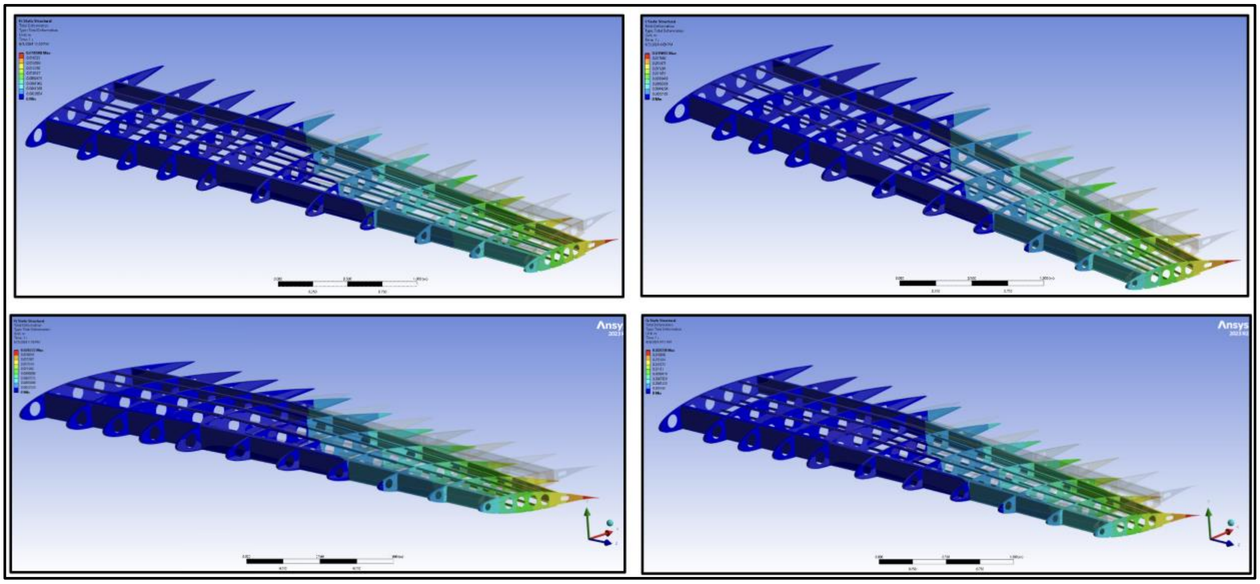

Figure 13: *Total Deformation Results for each Grid size. (Top Left: Grid 1, Top Right: Grid 2, Bottom Left: Grid 3, Bottom Right: Grid 4.)*

The **Figure 13** illustrates the total deformation results for each grid size for the quadratic tetrahedron element.

The difference in results from using the two types of elements is highly notable. This is because the linear tetrahedron uses linear shape functions, whereas the quadratic tetrahedron element uses quadratic shape functions. Thus, linear elements are a source of high error and reduced computational accuracy. On the other hand, the quadratic elements can better capture the curvature and more complex variations in the displacement field.

5. Grid Independent Study

The last step of conducting a static structural analysis, is to perform a grid independent study also known as mesh independent study. The grid independence study enables the static structural solution (deformation, stress strain, etc.) to be independent of the geometry's grid/mesh size. Therefore, a grid independent solution can lead to much accurate and reliable results for the structural analysis of large and complex geometries. The grid independent study further helps in validating the stability of the solution by calculating its steady, and stable value as the mesh is refined at each trial.

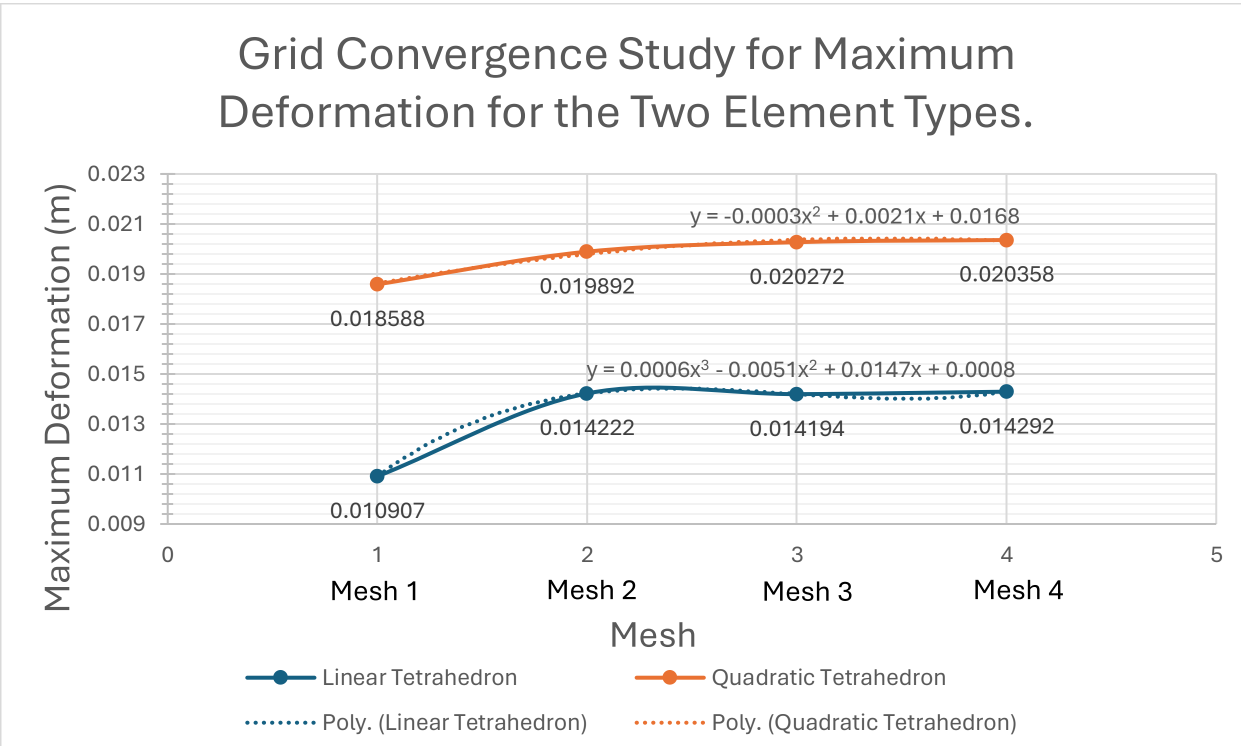

Figure 14: *Grid Convergence Study for Maximum Deformation for the Two Element Types.*

The study uses three mesh sizes to extrapolate a converging steady solution. The **Figure 14** above illustrates the convergence of the maximum deformation for the two element types for this project. Therefore, the grid independent study for this project confirms a grid independent solution for maximum deformation to be 0.020358 m and 0.014292 m for quadratic and linear tetrahedron elements respectively.

6. Discussion

This project aims to conduct a static structural analysis of a Cessna 152's wing structure. Throughout this study, the Cessna 152' wing structure has been simplified within reason to depict the actual behaviour of the wing structure during static conditions. However, these simplifications can be a source of inherent error on the wing model while calculating its deformation, stress, and strain values. For example, these errors are responsible for an inaccurate analysis of the connection points between the structural elements of the wing.

Furthermore, the types of wing loading used for this study does not account for any dynamic effects like turbulence, gust loads, cyclic loading, and transient aerodynamic forces. The boundary conditions for this study includes a fixed support at the fuselage-wing interface, and a wing strut simplified pin attachment. However, in reality the attachments have some degree of freedom for joint slipping which can alter the load distribution. The struct connection point is simple enough that it cannot analyze all the complexities of the actual load transfer.

7. Future Tasks

The next step in this project is to conduct a modal analysis on the wing structure to determine the mode shapes under the respective boundary conditions. The modal analysis helps in a better understanding of the dynamic behaviour of the wing structure by identifying the model's mode shapes, natural frequencies, and dampening characteristics.

Furthermore, a wing skin element can be added to the wing model to calculate the shear, bending, and torsional forces on its surface. Additionally, an optimal skin thickness and rib-stringer-skin connection procedures can be analyzed that reduces the stress level at these connection points while maximizing the force distribution.

8. Conclusion

In conclusion, the comprehensive design and analysis of the Cessna 152 wing structure have demonstrated that the wing is capable of withstanding various aerodynamic and structural loads with a significant safety margin. The use of both linear and quadratic tetrahedron elements in the finite element analysis provided a robust and thorough evaluation of the wing's performance under maximum loading conditions. The results showed that the maximum deformation and stress values are well within the material's failure limits, affirming the structural integrity and reliability of the wing design. This study confirms that the Cessna 152 wing structure is both robust and efficient, capable of ensuring passenger safety and operational performance while optimizing material usage. These findings contribute valuable insights for future wing design and optimization in the aviation industry.

9. References

1. P. V. Kumar, I. R. Raj, M. S. Reddy, and N. S. Prasad, "Design and Finite Element Analysis of Aircraft Wing using Ribs and Spars," Turkish journal of computer and mathematics education, vol. 12, no. 8, pp. 3224–3230, 2021.
2. Model 152 Series Cessna - Service Manual.
3. 'NACA 2412 (naca2412-il)'. Accessed: May 23, 2024. [Online]. Available: http://airfoiltools.com/airfoil/details?airfoil=naca2412-il
4. J. Shupek, "Cessna 152," Cessna 152 Aerobat, single-engine two-seat high-wing aerobatic-capable monoplane, USA, https://www.skytamer.com/Cessna_152.html (accessed May 23, 2024).
5. "Griggs aircraft refinishing," Griggs Aircraft Refinishing | Aux Fuel System STCs, http://griggsaircraft.com/fabrication/aux_fuel_systems (accessed May 23, 2024).
6. "Cessna 172 Skyhawk Aircraft Dimensions & Drawings," RSS, https://www.dimensions.com/element/cessna-172-skyhawk-aircraft (accessed May 23, 2024).

10. Appendix

Mesh 1

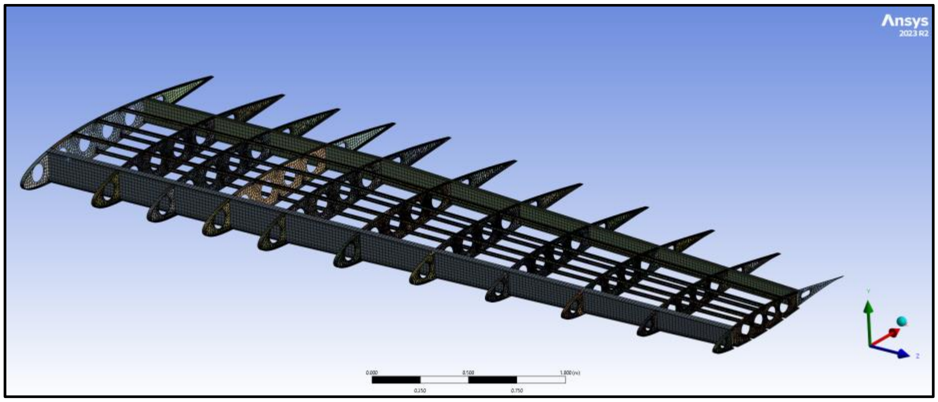

Figure 15: *Mesh 1.*

Mesh 2

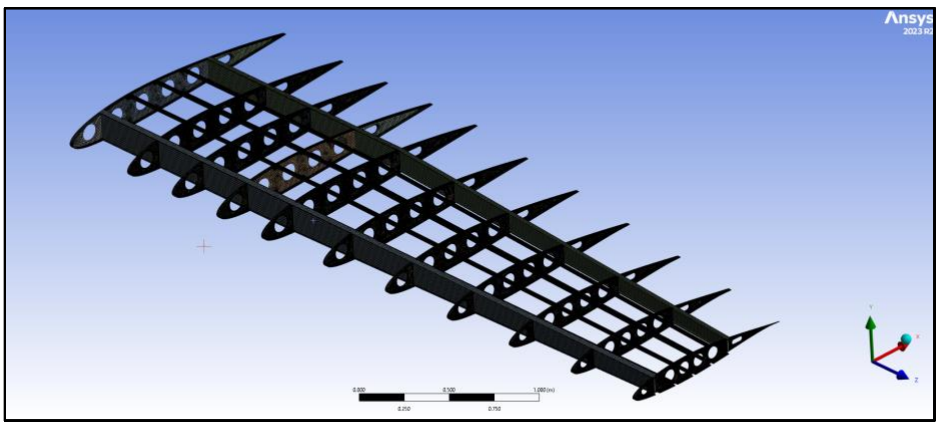

Figure 16: *Mesh 2.*

Mesh 3

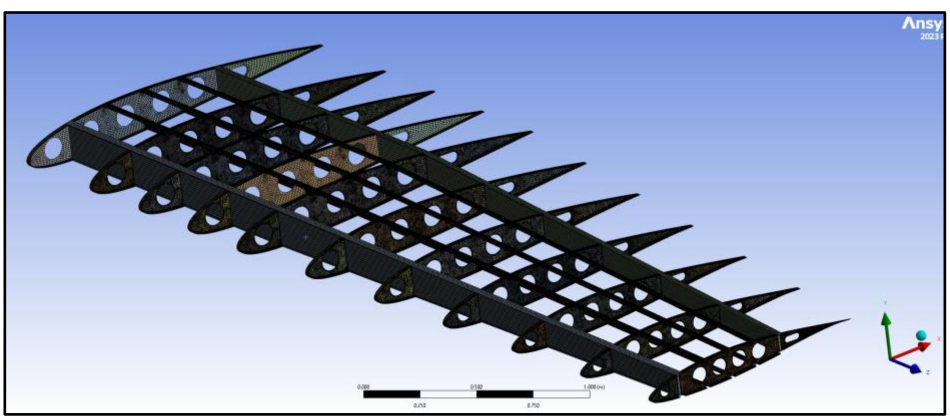

Figure 17: *Mesh 3.*

Mesh 4

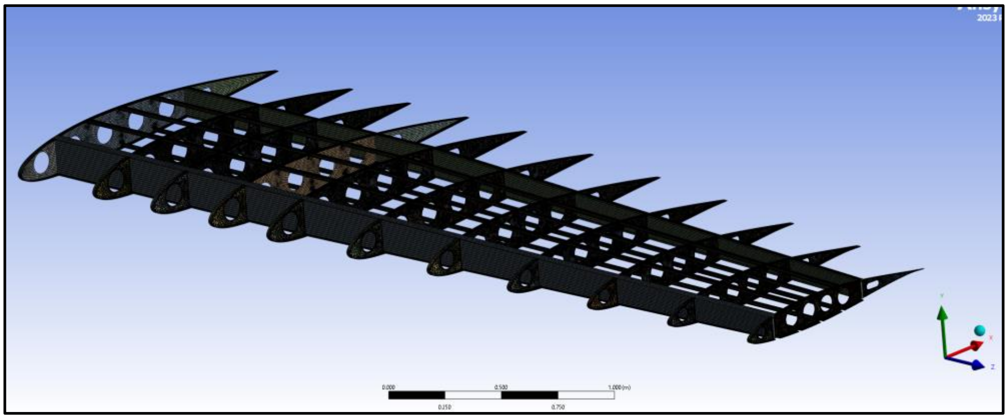

Figure 18: *Mesh 4.*

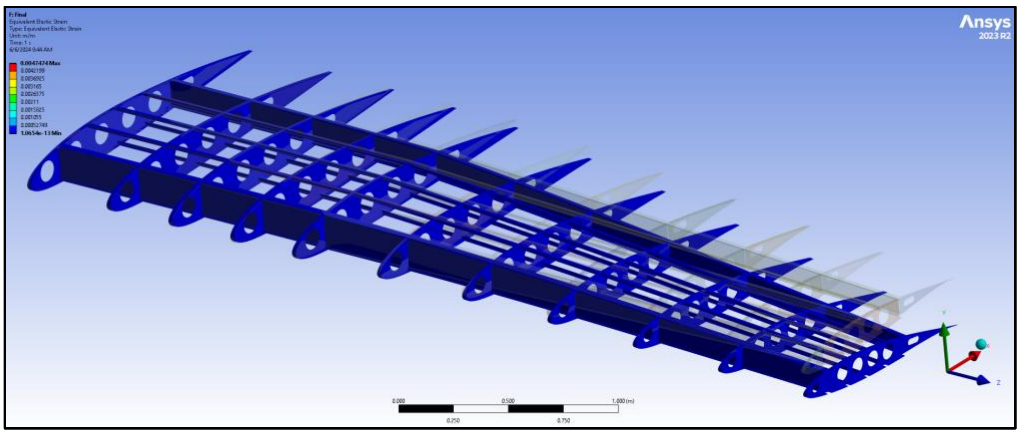

Figure 19: *Mesh 1, Linear Element, Strain.*

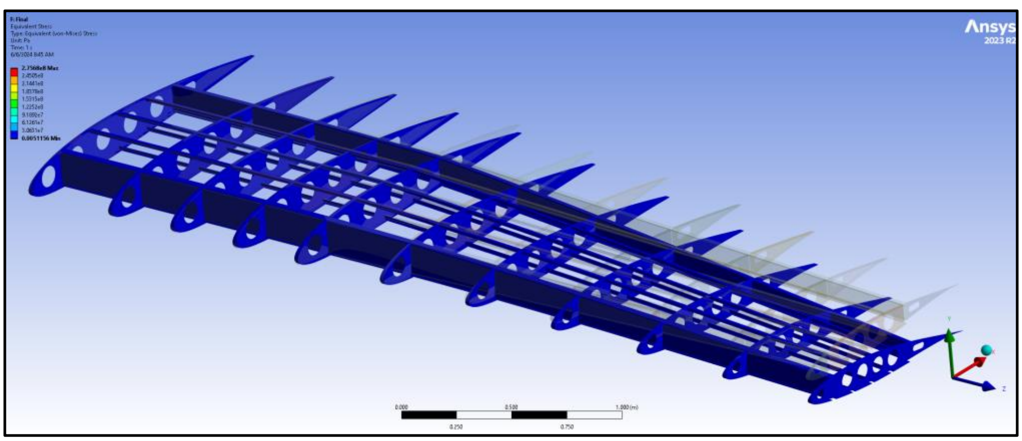

Figure 20: *Mesh 1, Linear Element, Stress.*

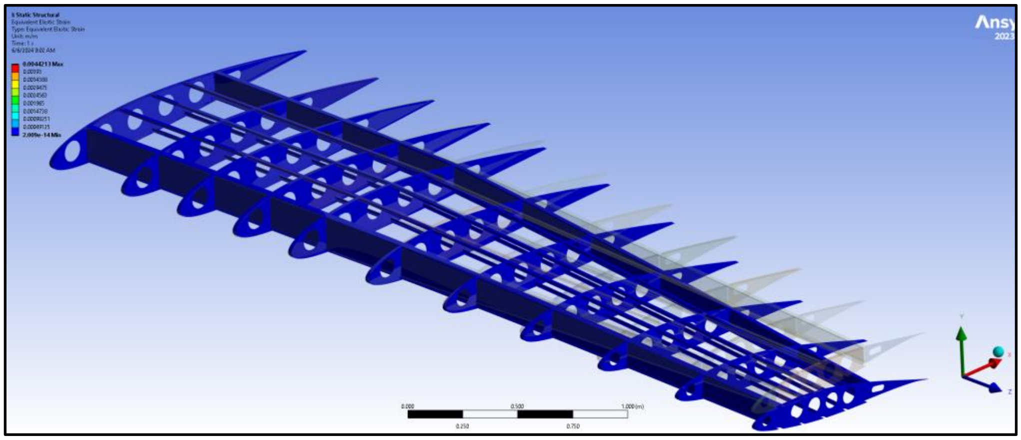

Figure 21: *Mesh 2, Linear Element, Strain.*

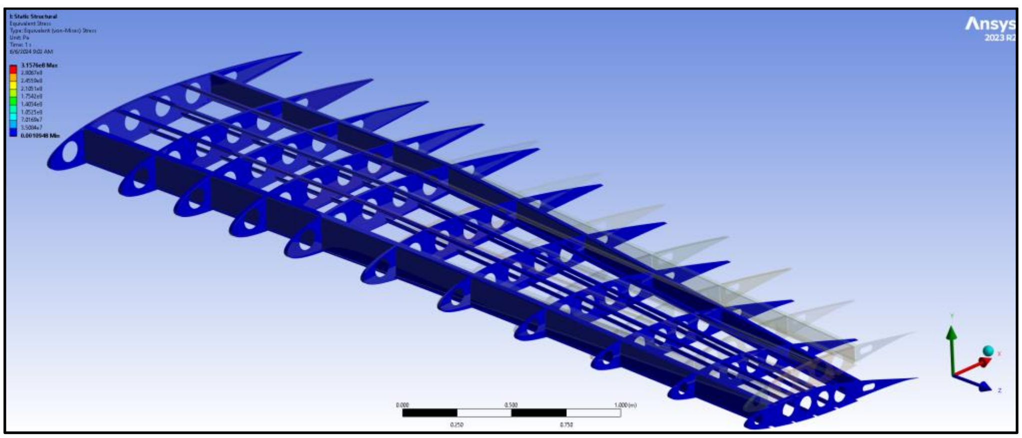

Figure 22: *Mesh 2, Linear Element, Stress.*

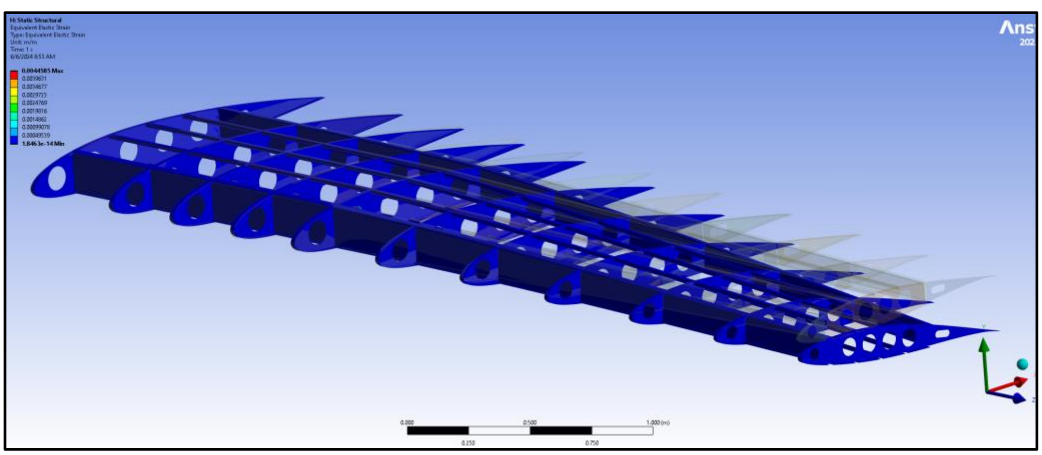

Figure 23: *Mesh 3, Linear Element, Strain.*

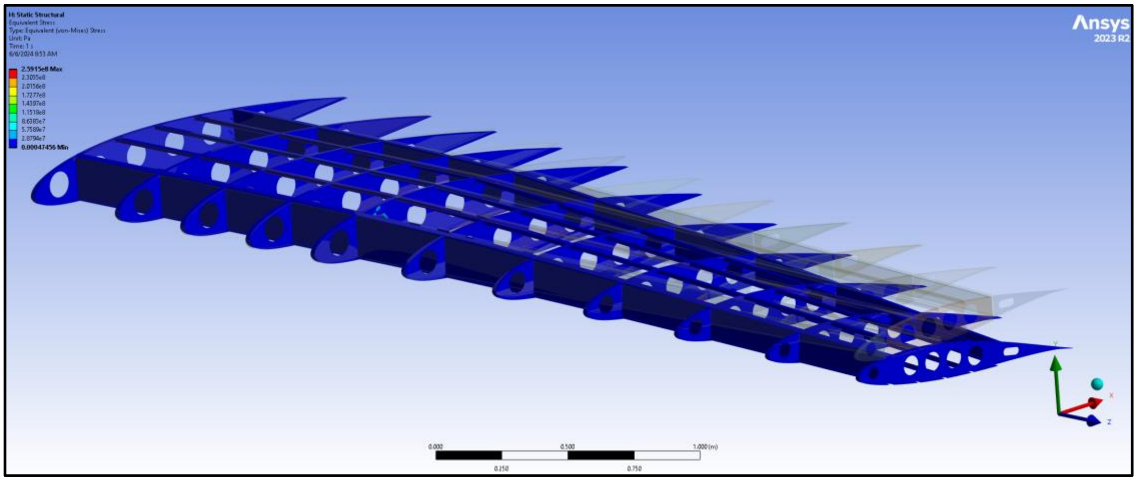

Figure 24: *Mesh 3, Linear Element, Stress.*

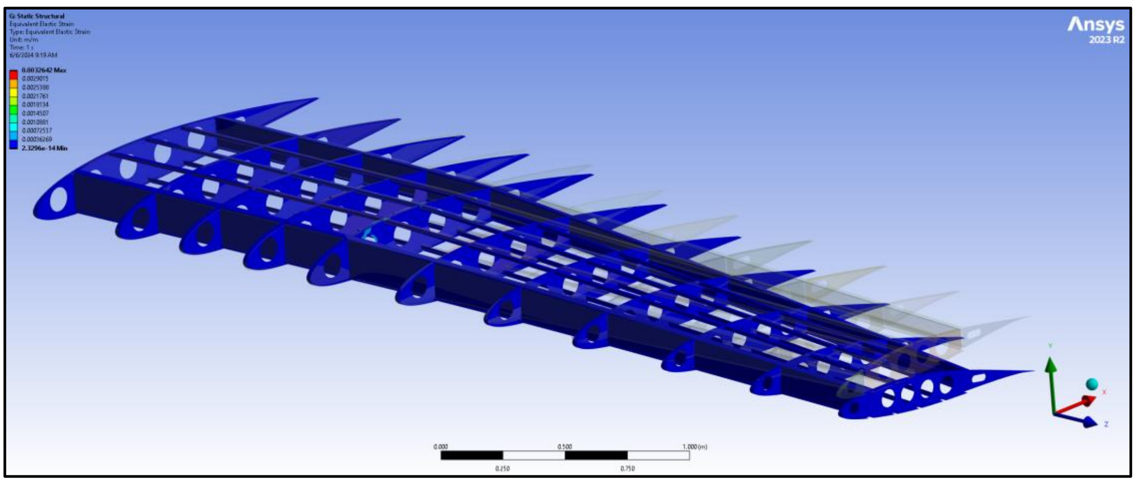

Figure 25: *Mesh 4, Linear Element, Strain.*

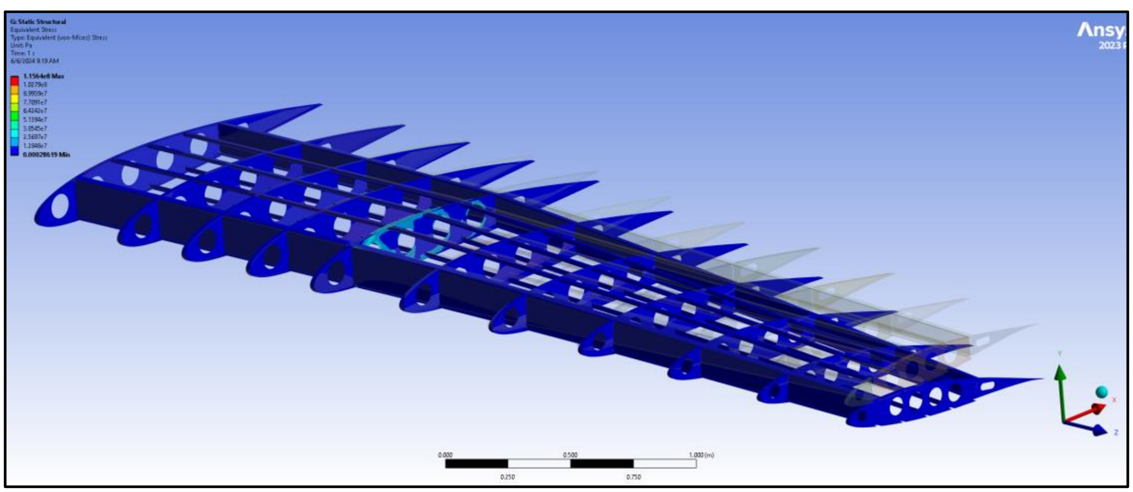

Figure 26: *Mesh 4, Linear Element, Stress.*

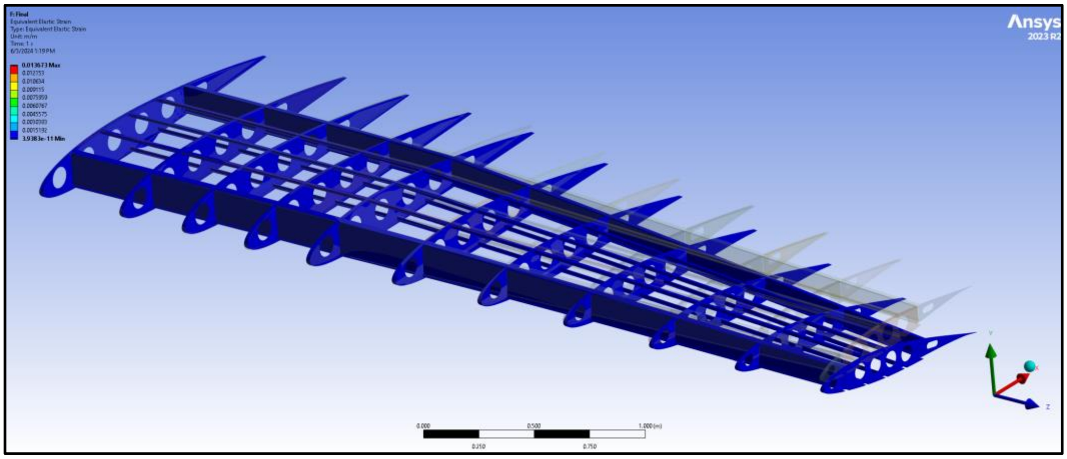

Figure 27: *Mesh 1, Quadratic Element, Strain.*

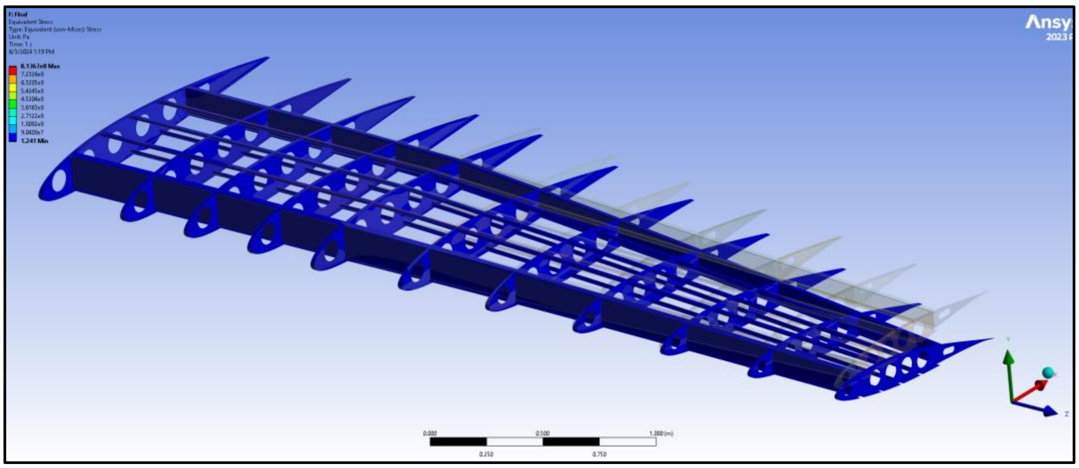

Figure 28: *Mesh 1, Quadratic Element, Stress.*

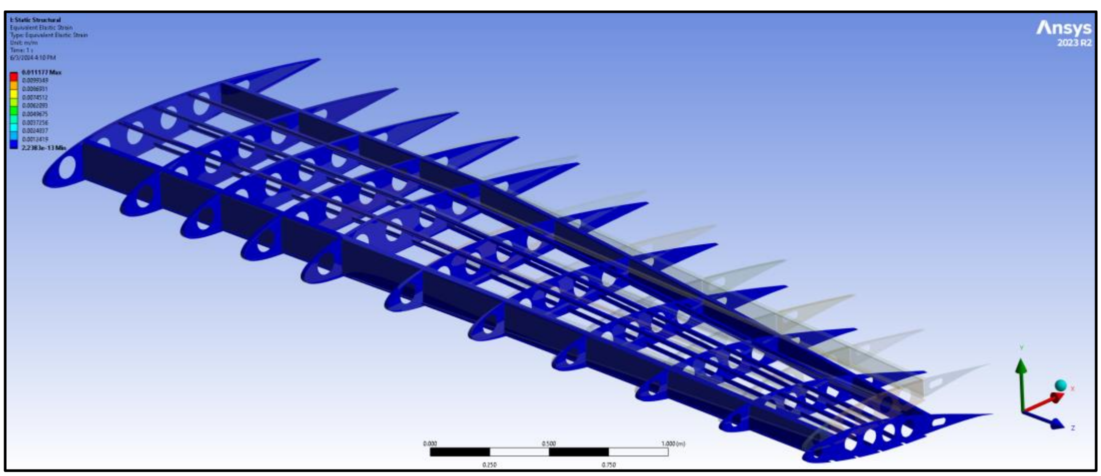

Figure 29*: Mesh 2, Quadratic Element, Strain.*

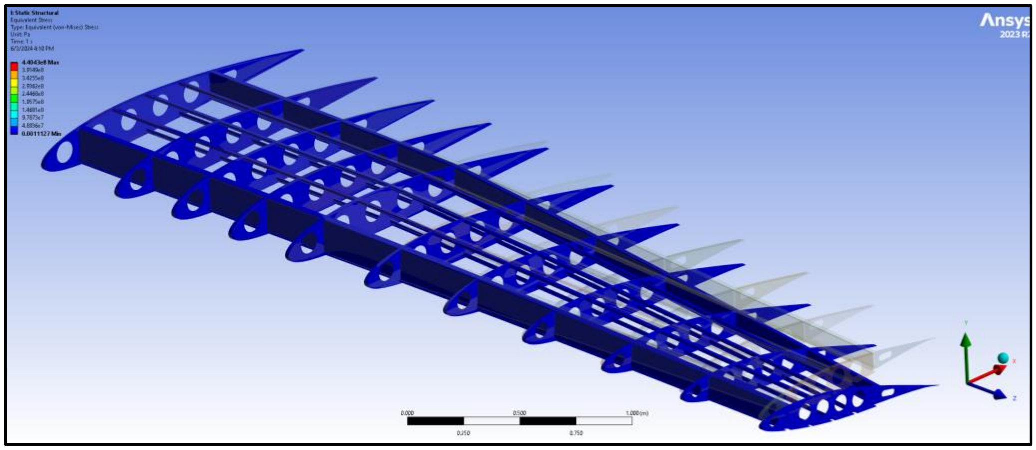

***Figure 30**: Mesh 2, Quadratic Element, Stress.*

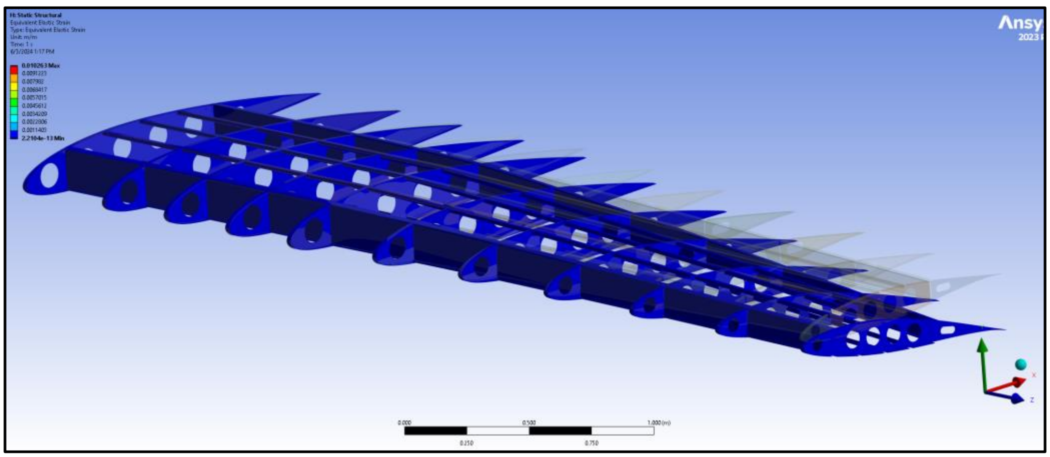

***Figure 31**: Mesh 3, Quadratic Element, Strain.*

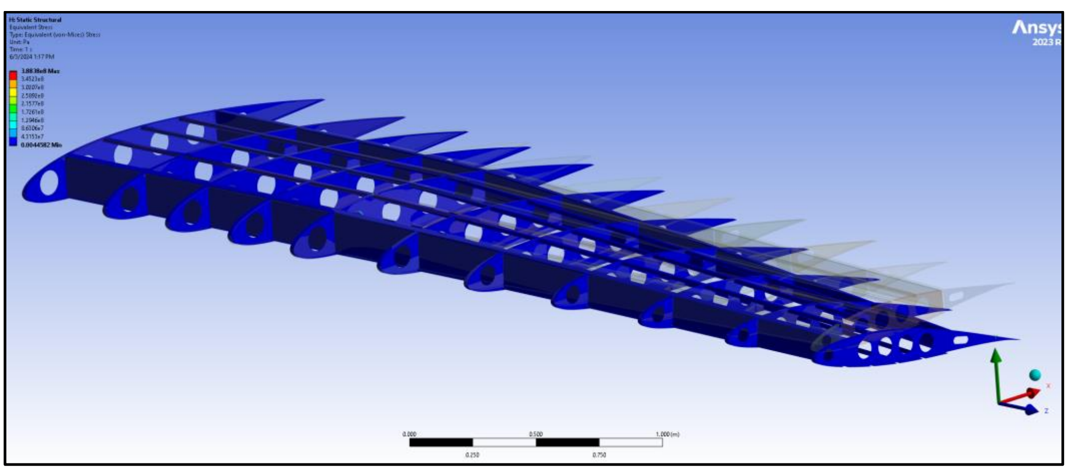

***Figure 32:** Mesh 3, Quadratic Element, Stress.*

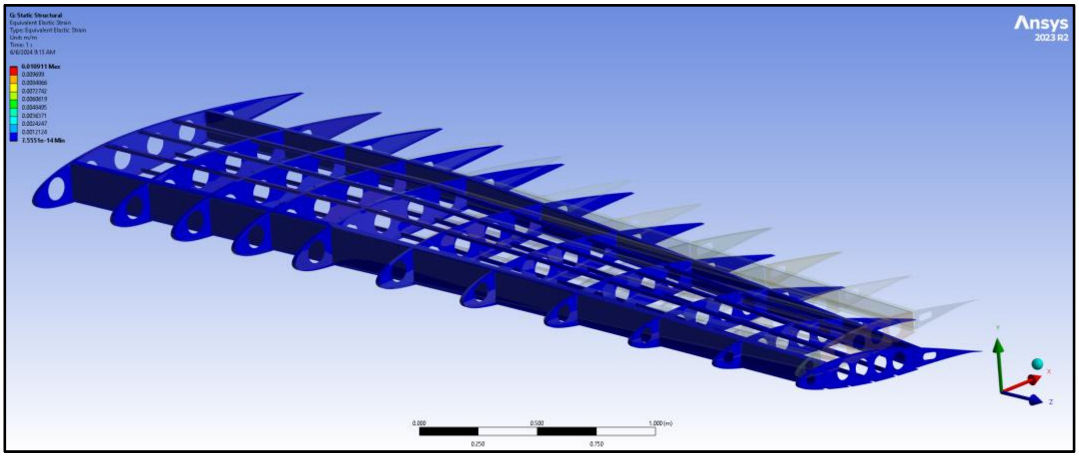

Figure 33: *Mesh 4, Quadratic Element, Strain.*

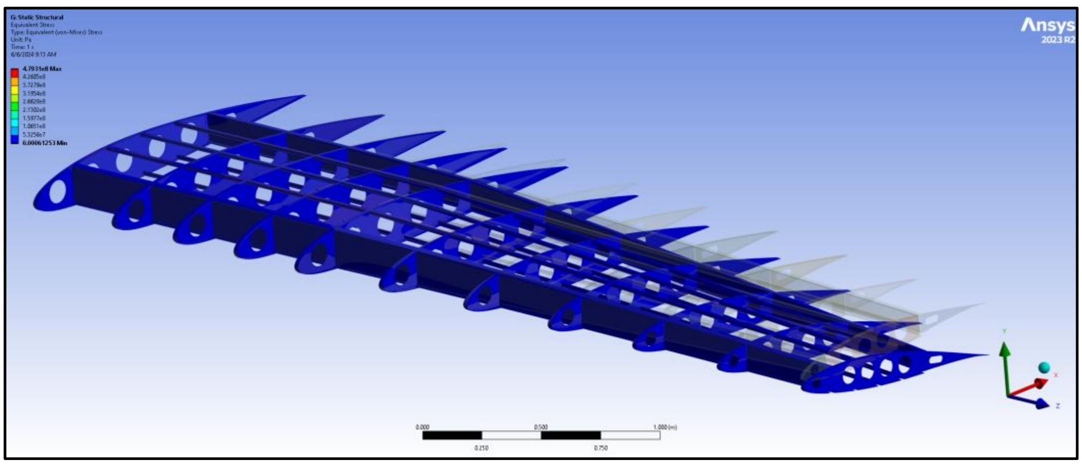

Figure 34: *Mesh 4, Quadratic Element, Stress.*